Journal of Statistics & Management Systems
ISSN 0972-0510 (Print), ISSN 2169-0014 (Online)
Vol. 27 (2024), No. 6, pp. 1117–1137
DOI : 10.47974/JSMS-1192

A time-delay model for the population dynamics of diabetes during pregnancy

Noorehan Yaacob
Hanis Nasir *
Department of Mathematical Sciences
Faculty of Science
Universiti Teknologi Malaysia
Johor Bahru 81310
Johor
Malaysia

Abstract

We studied a delay differential equations model for the population dynamics of diabetes during pregnancy. We considered four variables, namely women who are non-diabetic, women who are diabetic, women with gestational diabetes, and women with gestational diabetes and diabetes-related complications. We investigated the stability analysis of the equilibrium point by deriving of the transcendental characteristic equation. The numerical diagrams are visualized to verify the theoretical results. We further investigated the sensitivity analysis with respect to the equilibrium point. The normalized forward sensitivity indices suggested the critical and sensitive model inputs that capable of being handled to tackle the problems of diabetes during pregnancy.

Subject Classification: *92B05, 34D32, 35B35.*

Keywords: *Gestational diabetes, Time delay, Stability analysis, Sensitivity analysis.*

1. Introduction

Diabetes among expectant mothers is common these days. Cases of diabetes during pregnancy have shown an increase over the years [1, 2]. Diabetes during pregnancy can be categorized into two types. The first one is due to pre-existing type 1 diabetes, which the type 1 diabetes develops before pregnancy. The second one is due to pre-existing type 2 diabetes and is called gestational diabetes mellitus [3, 4]. Gestational

* *E-mail:* `hanisnasir20@gmail.com`

diabetes is one of the serious pregnancy complications. Gestational diabetes arises from factors such as obesity, maternal age, and family history [5]. Nevertheless, gestational diabetes is increasingly acknowledged as a possibility for preventative steps of type 2 diabetes and other diseases throughout a person's life. Gestational diabetes might have contributed for up to 30% of cases of type 2 diabetes [6].

Diabetes mellitus during pregnancy is a significant international health concern that contributes to many unpleasant outcomes. Then, Mat Daud et al. [7] developed and analyzed a mathematical model of the population dynamics of diabetes during pregnancy. Mat Daud et al. [7] considered four time-dependent variables, namely the women who are non-diabetic, women who are diabetic, women with gestational diabetes, and women with gestational diabetes and diabetes-related complications. Besides, the study of time delay has sparked significant fascination in ecosystems, where time delay can be used to designate the time required for young predators to mature [8] and the time delay in producing offspring [9]. In addition, many studies on diabetes population dynamics or time delays can be found in [10, 11, 12].

We organize this manuscript into the following sections. Section 2 discusses the model formulation of the population dynamics of gestational diabetes with time delay. In Section 3, we specify a critical delay $\tau_0 > 0$ of the time delay τ as a way that the equilibrium point P^* is locally asymptotically stable for $\tau \in [0, \tau_0)$ and unstable for $\tau > \tau_0$. A Hopf bifurcation occurs at P^* when $\tau = \tau_0$. We also discuss a method to determine the sensitive model inputs to change the equilibrium point P^* in Section 4. Lastly, we present the discussion and conclusion in Sections 5 and 6, respectively.

2. The mathematical model

In 2020, Mat Daud et al. [7] established a four-state population model to monitor the number of pregnant women with diabetes. The childbearing age is usually from 15 to 44 years old [13, 14]. The population of women in the childbearing age group is divided into four states: $V(t)$, $N(t)$, $K(t)$, and $G(t)$ (see Table 1 for the definition). The governing equations are as follows:

Table 1
The variables in model (2.1).

Variable	Definition
$V(t)$	The figure of women who are non-diabetic at time t.
$N(t)$	The figure of women who are diabetic at time t.
$K(t)$	The figure of women with gestational diabetes at time t.
$G(t)$	The figure of women with gestational diabetes and diabetes-related complications at time t.

$$\frac{dV(t)}{dt} = \Psi - (\mu + \sigma + \xi + \alpha)V(t) + \eta K(t) + \rho G(t), V(0) = V_0 > 0, \tag{2.1a}$$

$$\frac{dN(t)}{dt} = \varpi - (\varepsilon + \kappa + \Omega + \mu)N(t) + \sigma V(t) + \chi K(t) + \gamma G(t), N(0) = N_0 > 0, \tag{2.1b}$$

$$\frac{dK(t)}{dt} = \alpha V(t) + \Omega N(t) - (\eta + \chi + \omega + \nu + \delta)K(t), K(0) = K_0 > 0, \tag{2.1c}$$

$$\frac{dG(t)}{dt} = \omega K(t) - (\rho + \gamma + \theta + \beta)G(t), G(0) = G_0 > 0. \tag{2.1d}$$

The definition of all parameters in model (2.1) is given in Table 2. Mat Daud et al. [7] investigated model (2.1) for the non-negativity of the solution, local stability, and sensitivity analysis of the long-term solution.

In the present paper, we extend model (2.1) by considering a time delay in the development of diabetes from the point of non-diabetes. The progression of diabetes is slow and should include time delays [10]. A non-diabetic person may pass through an extensive pre-diabetes phase before becoming a full-blown diabetic [15, 16]. Then, the new model with time delay is as follows:

$$\frac{dV(t)}{dt} = \Psi - (\mu + \alpha + \xi)V(t) - \sigma V(t - \tau) + \eta K(t) + \rho G(t), \tag{2.2a}$$

$$\frac{dN(t)}{dt} = \varpi - (\varepsilon + \kappa + \Omega + \mu)N(t) + \sigma V(t - \tau)e^{-(\mu+\xi)\tau} + \chi K(t) + \gamma G(t), \tag{2.2b}$$

$$\frac{dK(t)}{dt} = \alpha V(t) + \Omega N(t) - (\eta + \chi + \omega + \nu + \delta)K(t), \tag{2.2c}$$

$$\frac{dG(t)}{dt} = \omega K(t) - (\rho + \gamma + \theta + \beta)G(t), \tag{2.2d}$$

where τ is the slow progression from non-diabetic to diabetic and the term $e^{-(\mu+\xi)\tau}$ is the proportion of $\sigma V(t - \tau)$ individuals who are still alive from time t to $t + \tau$. Figure 1 shows the compartmental layout of model (2.2). Furthermore, we consider the initial conditions for model (2.2) as follows:

Table 2

The definition of parameters in model (2.1).

Parameter	Definition
Ψ	The entry rate of women who are non-diabetic into the childbearing age group.
μ	The fatality rate due to causes other than diabetes.
ξ	The removal rate of women without diabetes from the childbearing age group.
σ	The rate of developing diabetes.
ε	The removal rate of women with diabetes from the childbearing age group.
κ	The diabetes-related death rate among women with diabetes.
ϖ	The entry rate of women with diabetes into the childbearing age group.
γ	The recovery rate of diabetes-related complications but remain to be diabetics in the non-pregnant state.
β	The diabetes-related death rate among women with gestational diabetes and diabetes-related complications.
θ	The death rate due to causes other than diabetes-related complications among women with gestational diabetes and diabetes-related complications.
ω	The rate of women with gestational diabetes developing diabetes-related complications.
χ	The rate of women with gestational diabetes who continue being diabetic in the non-pregnant state.
Ω	The rate of women with diabetes getting pregnant.
ν	The death rate of women with gestational diabetes due to causes other than diabetes.
δ	The diabetes-related death rate among women with gestational diabetes.
α	The rate of women who are non-diabetic getting pregnant with gestational diabetes.
η	The rate of women with gestational diabetes becoming non-diabetic after puerperium.
ρ	The recovery rate of diabetes-related complications and becoming non-diabetic in the non-pregnant state.

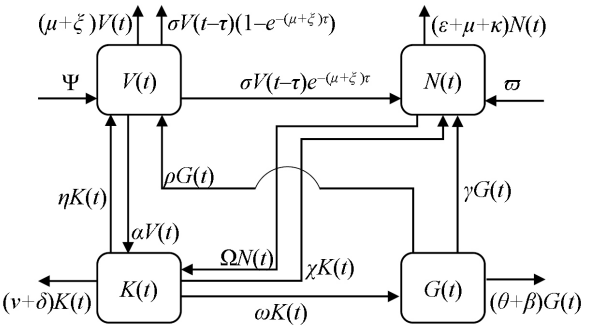

Figure 1

Compartmental diagram of diabetes during pregnancy.

$$V(\theta_1)=\phi(\theta_1)>0, \theta_1\in[-\tau,0],\ N(0)=N_0>0, K(0)=K_0>0, G(0)=G_0>0, \tag{2.3}$$

where $\phi(\theta_1)$ is a continuous function on $\theta_1\in[-\tau,0]$. By the fundamental theory of delay differential equations [17], we can easily show that the delayed model (2.2) with the initial conditions (2.3) has a unique solution.

2.1 *Non-negativity and boundedness of the solution*

Since the model monitors a human population, it is important to show that every variable is non-negative for time $t\geq 0$. If it is not, we identify the condition for which the solution will remain non-negative over time. In addition, resources are finite, so it is important to prove the boundedness of the solution.

Proposition 1: If condition:

(H1) $\Psi+\eta K(t_1)+\rho G(t_1)\geq \sigma V(t_1-\tau)$ at the boundary $V(t_1)=0$ for any time t_1, is satisfied, the solution of model (2.2) remains non-negative and bounded for $t\geq 0$. Furthermore, the set:

$$\hat{\Omega}=\left\{(V(t),N(t),K(t),G(t))\in\mathbb{R}^4_+ \mid V(t)+N(t)+K(t)+G(t)\leq\frac{\Psi+\varpi}{\hat{\varepsilon}}\right\},$$

where $\hat{\varepsilon}=\min\{(\theta+\beta),(v+\delta),(\varepsilon+\mu+\kappa),(\mu+\xi)\}$, is a positively-invariant set with respect to model (2.2).

Proof: For the non-negativity problem, we first investigate equation (2.2a). Equation (2.2a) can be written as

$$\frac{dV(t)}{dt} + (\mu + \xi + \alpha)V(t) = \Psi - \sigma V(t-\tau) + \eta K(t) + \rho G(t). \tag{2.4}$$

Multiplying equation (2.4) with $e^{(\mu+\xi+\alpha)t}$ yields

$$\frac{d}{dt}(V(t)e^{(\mu+\xi+\alpha)t}) = (\Psi + \eta K(t) + \rho G(t) - \sigma V(t-\tau))e^{(\mu+\xi+\alpha)t}. \tag{2.5}$$

By changing the independent variable of equation (2.5) from t to ε and integrating it from $\varepsilon = 0$ to $\varepsilon = t$, we obtain

$$V(t) = V(0)e^{-(\mu+\xi+\alpha)t} + e^{-(\mu+\xi+\alpha)t}\int_0^t (\Psi + \eta K(\varepsilon) + \rho G(\varepsilon) - \sigma V(\varepsilon-\tau))e^{(\mu+\xi+\alpha)\varepsilon}\, d\varepsilon. \tag{2.6}$$

Note that the integral term in equation (2.6) can become negative. If the solution of equation (2.2a) touches the boundary $V(t_1) = 0$ at any time t_1, equation (2.2a) becomes

$$\frac{dV(t_1)}{dt} = \Psi + \eta K(t_1) + \rho G(t_1) - \sigma V(t_1 - \tau).$$

Then, if $\Psi + \eta K(t_1) + \rho G(t_1) < \sigma V(t_1 - \tau)$, then the solution of equation (2.2a) enters the negative region (see Figure 2). To avoid obtaining a negative solution of equation (2.2a), condition (H1) needs to be satisfied. This condition (H1) suggests that $V(t)$ remains non-negative for $t \geq 0$.

Next, we investigate equation (2.2b). We claim that $N(t)$ remains positive for $t \geq 0$. On the contrary, we assume there is a first time $\hat{t} > 0$ such that the solution of equation (2.2b) touches zero where $N(\hat{t}) = 0$ and $(K(\hat{t}), G(\hat{t})) > (0,0)$. Then, equation (2.2b) becomes

$$\frac{dN(\hat{t})}{dt} = \varpi + \sigma V(\hat{t} - \tau)e^{-(\mu+\xi)\tau} + \chi K(\hat{t}) + \gamma G(\hat{t}) > 0.$$

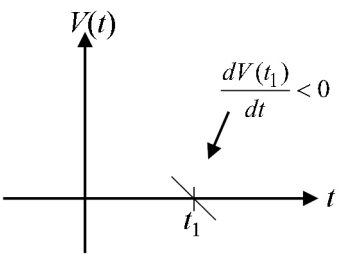

Figure 2
The slope of $\frac{dV(t_1)}{dt} < 0$.

Hence, $N(t) < 0$ for $t \in (\hat{t} - \varepsilon, \hat{t})$ where $\varepsilon > 0$ is sufficiently small. This contradicts our initial claim where $N(t) > 0$ for $t \in [0, \hat{t})$. Consequently, $N(t)$ remains non-negative for $t \geq 0$.

Similarly, the non-negativity of variables $K(t)$ and $G(t)$ can be proved in the same way as the proof of variable $N(t)$.

For the boundedness problem, we denote the total population $T(t) = V(t) + N(t) + K(t) + G(t)$. It follows that

$$\frac{dT(t)}{dt} = \Psi + \varpi - (\theta + \beta)G(t) - (\nu + \delta)K(t) - (\varepsilon + \mu + \kappa)N(t) - (\mu + \xi)V(t) - \sigma V(t - \tau)(1 - e^{-(\mu+\xi)\tau}). \tag{2.7}$$

By condition (H1) and the non-negativity of every variable, equation (2.7) becomes

$$\frac{dT(t)}{dt} \leq \Psi + \varpi - \hat{\varepsilon} T(t).$$

Then, we can obtain

$$T(t) \leq \frac{\Psi + \varpi}{\hat{\varepsilon}} + \left(T(0) - \frac{\Psi + \varpi}{\hat{\varepsilon}} \right) e^{-\hat{\varepsilon} t}.$$

We have $T(t) \leq \frac{\Psi + \varpi}{\hat{\varepsilon}}$ for $T(0) < \frac{\Psi + \varpi}{\hat{\varepsilon}}$. This indicates the upper bound of the total population size is $\frac{\Psi + \varpi}{\hat{\varepsilon}}$. Condition (H1) is required to be true so that the set $\hat{\Omega}$ becomes a positively-invariant set for model (2.2).

The set $\hat{\Omega}$ is considered as our feasible region and the equilibrium point is within this region whenever it exists.

3. Stability analysis of the equilibrium point

The equilibrium point of model (2.2), $P^* = (V^*, N^*, K^*, G^*)$, is the long-term solution in which it occurs when all rates of changes are zero. For a large time t, we have

$$V(t) = V(t - \tau) = V^*, N(t) = N^*, K(t) = K^*, G(t) = G^*. \tag{3.1}$$

By substituting (3.1) into the right-hand-side equations of model (2.2) and letting them equal to zero, we obtain:

$$\Psi - a_1 V^* + \eta K^* + \rho G^* = 0, \tag{3.2a}$$

$$\varpi - a_2 N^* + \sigma V^* e^{-(\mu+\xi)\tau} + \chi K^* + \gamma G^* = 0, \tag{3.2b}$$

$$\alpha V^* + \Omega N^* - a_3 K^* = 0, \tag{3.2c}$$

$$\omega K^* - a_4 G^* = 0, \tag{3.2d}$$

where

$$a_1 = \mu + \sigma + \xi + \alpha, \quad a_2 = \varepsilon + \kappa + \Omega + \mu,$$
$$a_3 = \eta + \chi + \omega + \nu + \delta, \quad a_4 = \rho + \gamma + \theta + \beta,$$

By solving system (3.2) simultaneously, we obtain a unique point $P^* = (V^*, N^*, K^*, G^*)$ such that:

$$V^* = \frac{a_3 a_4 (a_5 \Psi + \eta \Omega a_4 \varpi + \rho \omega \Omega \varpi)}{a_6 + \sigma \Omega a_3 a_4 (\eta a_4 + \rho \omega)(1 - e^{-(\mu+\xi)\tau}) + a_7 (\sigma a_3 a_4 + \alpha \chi a_4 + \alpha \omega \gamma)},$$
$$N^* = a_5^{-1}[a_3 a_4 \varpi + (a_3 a_4 \sigma e^{-(\mu+\xi)\tau} + a_4 \chi \alpha + \gamma \omega \alpha) V^*],$$
$$K^* = \frac{\alpha V^* + \Omega N^*}{a_3},$$
$$G^* = \frac{\omega K^*}{a_4},$$

where

$$a_5 = a_2[(\rho + \theta + \beta)\omega + (\eta + \nu + \delta)a_4] + (\gamma \omega + a_4 \chi)(\varepsilon + \mu + \kappa),$$
$$a_6 = a_5[a_3 a_4 (\mu + \xi) + \alpha a_4 (\nu + \delta) + \alpha \omega (\theta + \beta)],$$
$$a_7 = (\varepsilon + \mu + \kappa)(\rho \omega + \eta a_4 + \gamma \omega + a_4 \chi) + a_2[(\theta + \beta)\omega + (\nu + \delta)a_4].$$

Since $e^{-(\mu+\xi)\tau} \in (0,1]$, the equilibrium point $P^* = (V^*, N^*, K^*, G^*)$ remains positive for the positive range of parameter values.

3.1 *Local stability*

To investigate the behavior of the solution near the equilibrium point P^*, we introduce

$$V(t) = V^* + u_1(t), N(t) = N^* + u_2(t), K(t) = K^* + u_3(t), G(t) = G^* + u_4(t),$$

where $\mathbf{u}(t) = [u_1(t), u_2(t), u_3(t), u_4(t)]^{\mathrm{T}}$ is a matrix of time-dependent functions that are relatively close to point P^*. The linearized system of model (2.2) at P^* is in the form of $\frac{d\mathbf{u}(t)}{dt} = \mathbf{J}_0 \mathbf{u}(t) + \mathbf{J}_\tau \mathbf{u}(t - \tau)$, where

$$\mathbf{J}_0 = \begin{bmatrix} -(\mu+\xi+\alpha) & 0 & \eta & \rho \\ 0 & -a_2 & \chi & \gamma \\ \alpha & \Omega & -a_3 & 0 \\ 0 & 0 & \omega & -a_4 \end{bmatrix}, \mathbf{J}_\tau = \begin{bmatrix} -\sigma & 0 & 0 & 0 \\ \sigma e^{-(\mu+\xi)\tau} & 0 & 0 & 0 \\ 0 & 0 & 0 & 0 \\ 0 & 0 & 0 & 0 \end{bmatrix}.$$

The corresponding characteristic equation is derived by computing $\det[\lambda \mathbf{I}_4 - \mathbf{J}_0 - e^{-\lambda\tau} \mathbf{J}_\tau] = 0$, where λ represents the eigenvalues and $\mathbf{I}_4$

denotes a 4-dimension identity matrix. Then, the characteristic equation is given by

$$\lambda^4 + z_1\lambda^3 + z_2\lambda^2 + z_3\lambda + z_4 + e^{-\lambda\tau}[\sigma\lambda^3 + z_5\lambda^2 + (z_6 + z_8)\lambda + (z_7 + z_9)] = 0, \quad (3.3)$$

where

$$\begin{aligned}
z_1 &= \mu + \xi + \alpha + a_2 + a_3 + a_4,\\
z_2 &= (a_2 + a_3)a_4 + (\varepsilon + \mu + \kappa)a_3 + \Omega(\eta + \omega + \nu + \delta)\\
&\quad + (\mu + \xi)(a_2 + a_3 + a_4) + \alpha(a_2 + \chi + \omega + \nu + \delta + a_4),\\
z_3 &= (\varepsilon + \mu + \kappa)a_3a_4 + \Omega(\eta + \nu + \delta)a_4 + \Omega\omega(\rho + \theta + \beta)\\
&\quad + (\mu + \xi)[(a_2 + a_3)a_4 + (\varepsilon + \mu + \kappa)a_3 + \Omega(\eta + \omega + \nu + \delta)]\\
&\quad + \alpha[\omega(\gamma + \theta + \beta) + (a_2 + \chi + \nu + \delta)a_4 + (\varepsilon + \mu + \kappa)\chi + a_2(\omega + \nu + \delta)],\\
z_4 &= (\mu + \xi)[(\varepsilon + \mu + \kappa)a_3a_4 + \Omega a_4(\eta + \nu + \delta) + \Omega\omega(\rho + \theta + \beta)]\\
&\quad + \alpha[\chi a_4 + \omega(\gamma + \theta + \beta)](\varepsilon + \mu + \kappa) + \alpha a_2a_4(\nu + \delta) + \alpha\Omega\omega(\theta + \beta),\\
z_5 &= \sigma(a_2 + a_3 + a_4),\\
z_6 &= \sigma[(a_2 + a_3)a_4 + (\varepsilon + \mu + \kappa)a_3 + \Omega(\omega + \nu + \delta)],\\
z_7 &= \sigma[(\varepsilon + \mu + \kappa)a_3a_4 + \Omega(\nu + \delta)a_4 + \Omega\omega(\theta + \beta)],\\
z_8 &= \sigma\Omega\eta(1 - e^{-(\mu+\xi)\tau}),\\
z_9 &= \sigma\Omega(\eta a_4 + \omega\rho)(1 - e^{-(\mu+\xi)\tau}).
\end{aligned}$$

Notice that $z_c > 0$ $(c = 1, 2, \ldots, 9)$ for the positive range of parameter values.

3.1.1 No time delay

Assume that $\tau = 0$. In this case, equation (3.3) becomes

$$\lambda^4 + (\sigma + z_1)\lambda^3 + (z_2 + z_5)\lambda^2 + (z_3 + z_6)\lambda + (z_4 + z_7) = 0. \quad (3.4)$$

Notice that $(\sigma + z_1) > 0$, $(z_2 + z_5) > 0$, $(z_3 + z_6) > 0$, and $(z_4 + z_7) > 0$. According to Corollary 4.1 in [18], all roots of equation (3.3) are negative or have negative real parts. Thus, we have the following theorem.

Theorem 1: *In the absence of delay, the equilibrium point P^* is locally asymptotically stable.*

3.1.2 The critical delay

For the case of $\tau > 0$, we need to show that the roots of equation (3.3) are not permitted to intersect the imaginary axis; that is, the characteristic

equation cannot have pure imaginary roots [19, 20]. Now, suppose that for some $\tau > 0$, there exists a number $\zeta > 0$ such that $\lambda = i\zeta$ $(i = \sqrt{-1})$ is one of the roots of equation (3.3). By substituting $\lambda = i\zeta$ into equation (3.3) and separating the real and imaginary parts, we obtain

$$\zeta^4 - z_2\zeta^2 + z_4 = (z_5\zeta^2 - (z_7 + z_9))\cos\zeta\tau + (\sigma\zeta^3 - (z_6 + z_8)\zeta)\sin\zeta\tau, \quad (3.5a)$$

$$z_1\zeta^3 - z_3\zeta = (z_5\zeta^2 - (z_7 + z_9))\sin\zeta\tau - (\sigma\zeta^3 - (z_6 + z_8)\zeta)\cos\zeta\tau. \quad (3.5b)$$

After we square and add the equations in (3.5), we obtain:

$$\zeta^8 + \varphi_1\zeta^6 + \varphi_2\zeta^4 + \varphi_3\zeta^2 + \varphi_4 = 0, \quad (3.6)$$

where

$$\begin{aligned}
\varphi_1 &= z_1^2 - 2z_2 - \sigma^2,\\
\varphi_2 &= z_2^2 + 2z_4 - 2z_1z_3 - z_5^2 + 2\sigma(z_6 + z_8),\\
\varphi_3 &= z_3^2 - 2z_2z_4 + 2z_5(z_7 + z_9) - (z_6 + z_8)^2,\\
\varphi_4 &= (z_4 + z_7 + z_9)(z_4 - z_7 - z_9).
\end{aligned}$$

Let $\Phi = \zeta^2$. Therefore, equation (3.6) can be written as

$$\Phi^4 + \varphi_1\Phi^3 + \varphi_2\Phi^2 + \varphi_3\Phi + \varphi_4 = 0. \quad (3.7)$$

Suppose that

(H2) $(\varphi_1, \varphi_2, \varphi_3, \varphi_4) > (0, 0, 0, 0)$.

This condition (H2) implies that all roots of equation (3.7) are negative or have negative real parts (based on Corollary 4.1 in [18]). This is a contradiction because $\zeta^2 = \Phi < 0$. Hence, the characteristic equation (3.3) cannot have $\lambda = i\zeta$ as one of the roots. The equilibrium point P^* is locally asymptotically stable for all $\tau \geq 0$.

Now, we assume that:

(H3) Equation (3.7) has at least one positive root.

WLOG, we consider that equation (3.7) has four positive roots given by Φ_1, Φ_2, Φ_3, and Φ_4. Then, equation (3.6) have four positive roots given by $\zeta_1 = \sqrt{\Phi_1}$, $\zeta_2 = \sqrt{\Phi_2}$, $\zeta_3 = \sqrt{\Phi_3}$, and $\zeta_4 = \sqrt{\Phi_4}$. For every ζ_k $(k = 1, 2, 3, 4)$, the corresponding critical delay is given by

$$\tau_k^{(j)} = \frac{1}{\zeta_k}\cos^{-1}\left\{\frac{\hat{\Phi}}{\hat{\varphi}}\right\} + \frac{2j\pi}{\zeta_k}, \quad j = 0, 1, 2, \ldots,$$

where

$$\hat{\Phi} = (\zeta_k^4 - z_2\zeta_k^2 + z_4)(z_5\zeta_k^2 - (z_7 + z_9)) - (z_1\zeta_k^2 - z_3)(\sigma\zeta_k^2 - (z_6 + z_8))\zeta_k^2,$$
$$\hat{\varphi} = (\sigma\zeta_k^3 - (z_6 + z_8)\zeta_k)^2 + (z_5\zeta_k^2 - (z_7 + z_9))^2.$$

Let $\tau_0 = \min_{k=1,2,3,4}\{\tau_k^{(0)}\}$ be the first critical delay at which equation (3.3) has a pair of complex conjugate roots and $\lambda = \pm i\zeta_0$ are denoted as the corresponding roots. Then, the equilibrium point P^* is locally asymptotically stable for $\tau \in [0, \tau_0)$.

In order to confirm the existence of Hopf bifurcation at $\tau = \tau_0$ [21], the following transversality condition must be satisfied:

$$\operatorname{sign}\left\{\Re\left[\frac{d\lambda(\tau)}{d\tau}\right]|_{\lambda(\tau_0)=i\zeta_0}\right\} > 0.$$

By differentiating equation (3.3) with respect to τ, we obtain

$$\begin{aligned}\left[\frac{d\lambda}{d\tau}\right]^{-1} &= (e^{\lambda\tau}(4\lambda^3 + 3z_1\lambda^2 + 2z_2\lambda + z_3) + 3\sigma\lambda^2 + 2z_5\lambda + (z_6 + z_8)\\ &\quad - \tau\sigma\lambda^3 - \tau z_5\lambda^2 - \tau(z_6 + z_8)\lambda - \tau(z_7 + z_9))\\ &\quad \times(\sigma\lambda^4 + z_5\lambda^3 + (z_6 + z_8)\lambda^2 + (z_7 + z_9)\lambda\\ &\quad - \lambda e^{-(\mu+\xi)\tau}\sigma\Omega\eta(\mu + \xi) - e^{-(\mu+\xi)\tau}\sigma\Omega(\eta a_4 + \omega\rho)(\mu + \xi))^{-1}.\end{aligned} \tag{3.8}$$

By substituting $\lambda(\tau_0) = i\zeta_0$ into equation (3.8), we obtain

$$\left[\frac{d\lambda}{d\tau}\right]^{-1}\Bigg|_{\lambda(\tau_0)=i\zeta_0} = \frac{f_1 + if_2}{f_3 + if_4}, \tag{3.9}$$

where

$$\begin{aligned}f_1 &= (\tau_0 z_5 - 3\sigma)\zeta_0^2 + (z_6 + z_8 - \tau_0 z_7 - \tau_0 z_9) - (3z_1\zeta_0^2 - z_3)\cos\zeta_0\tau_0 + (4\zeta_0^2 - 2z_2)\\ &\quad \zeta_0 \sin\zeta_0\tau_0,\\ f_2 &= \tau_0\sigma\zeta_0^3 + (2z_5 - \tau_0 z_6 - \tau_0 z_8)\zeta_0 - (4\zeta_0^2 - 2z_2)\zeta_0\cos\zeta_0\tau_0 - (3z_1\zeta_0^2 - z_3)\sin\zeta_0\tau_0,\\ f_3 &= \sigma\zeta_0^4 - (z_6 + z_8)\zeta_0^2 - e^{-(\mu+\xi)\tau_0}\sigma\Omega(\eta a_4 + \omega\rho)(\mu + \xi),\\ f_4 &= -z_5\zeta_0^3 + (z_7 + z_9)\zeta_0 - \zeta_0 e^{-(\mu+\zeta)\tau_0}\sigma\Omega\eta(\mu + \xi).\end{aligned}$$

The real part of equation (3.9) is given by

$$\Re\left[\frac{d\lambda}{d\tau}\right]^{-1}\Bigg|_{\lambda(\tau_0)=i\zeta_0} = \frac{f_1 f_3 + f_2 f_4}{f_3^2 + f_4^2}.$$

Suppose that

(H4) $f_1 f_3 + f_2 f_4 > 0.$

This condition (H4) implies that

$$\operatorname{sign}\left\{\Re\left[\frac{d\lambda}{d\tau}\right]^{-1}\Big|_{\lambda(\tau_0)=i\zeta_0}\right\}=\operatorname{sign}\left\{\Re\left[\frac{d\lambda}{d\tau}\right]\Big|_{\lambda(\tau_0)=i\zeta_0}\right\}>0.$$

The following theorem is established.

Theorem 2: *For model (2.2),*

(i) *if condition (H2) is satisfied, then the equilibrium point* P^* *is locally asymptotically stable for all* $\tau \geq 0$.

(ii) *if conditions (H3) and (H4) are satisfied, then the equilibrium point* P^* *is locally asymptotically stable for* $\tau \in [0, \tau_0)$ *and becomes unstable for* $\tau > \tau_0$. *Furthermore, a Hopf bifurcation occurs at* $\tau = \tau_0$ *and a family of periodic orbits bifurcates from* P^*.

3.2 *Validation of the theoretical results*

Numerical simulations are conducted to confirm the theoretical findings. For numerical examples, we consider four different sets of model inputs given in Table 3.

Table 3

Four sets of model inputs for the simulations of model (2.2).

Model input	(i) Set 1	(ii) Set 2	(iii) Set 3	(iv) Set 4
Ψ	10	10	10	10
μ	0.101	0.101	0.101	0.101
ξ	0.102	0.102	0.102	0.102
σ	0.1	0.1	0.5	0.5
ε	0.104	0.104	0.104	0.104
κ	0.105	0.105	0.105	0.105
ϖ	1	1	1	1
γ	0.107	0.107	0.107	0.107
β	0.108	0.108	0.108	0.108
θ	0.109	0.109	0.109	0.109
ω	0.11	0.11	0.11	0.11
χ	0.112	0.112	0.112	0.112
Ω	0.113	0.113	0.113	0.113
ν	0.114	0.114	0.114	0.114
δ	0.115	0.115	0.115	0.115
α	0.116	0.116	0.116	0.116

Contd...

η	0.117	0.117	0.117	0.117
ρ	0.118	0.118	0.118	0.118
ϕ	5	5	5	5
N_0	1	1	1	1
K_0	1	1	1	1
G_0	1	1	1	1
τ	0	1	1	5.8379

For the model inputs given in Table 3(i), the corresponding equilibrium point is $P^* = (26.5334,\ 11.1389,\ 7.6348,\ 1.9001)$. According to Theorem 1, the equilibrium point P^* is locally asymptotically stable (see Figure 3).

For the model inputs given in Table 3(ii), the corresponding equilibrium point is $P^* = (26.4391,\ 9.8799,\ 7.3651,\ 1.8329)$. Moreover, the corresponding coefficients of equation (3.7) are $\varphi_1 = 0.8411,\ \varphi_2 = 0.2344,\ \varphi_3 = 0.0242,$ and $\varphi_4 = 7.2483 \times 10^{-4}$. Then, condition (H2) is satisfied. According to Theorem 2(i), the equilibrium point P^* is locally asymptotically stable (see Figure 4).

For the model inputs given in Table 3(iii), the corresponding equilibrium point is $P^* = (13.3079,\ 17.2177,\ 6.1432,\ 1.5288)$. Moreover, the corresponding roots of equation (3.7) are $\Phi_1 = -0.3737,\ \Phi_2 = -0.2847,\ \Phi_3 = 0.1455,$ and $\Phi_4 = -0.0882$. Then, condition (H3) is satisfied and the critical delay $\tau_0 = 5.9083$. According to Theorem 2(ii), the equilibrium point P^* is locally asymptotically stable because $\tau = 1 < \tau_0$ (see Figure 5).

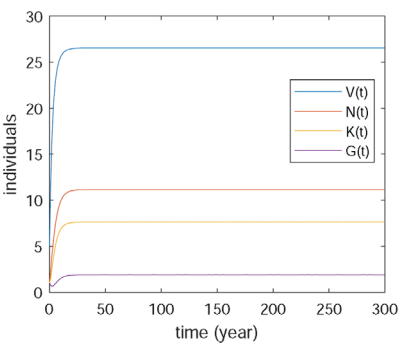

Figure 3

Simulation of model (2.2) with the model inputs in Table 3(i).

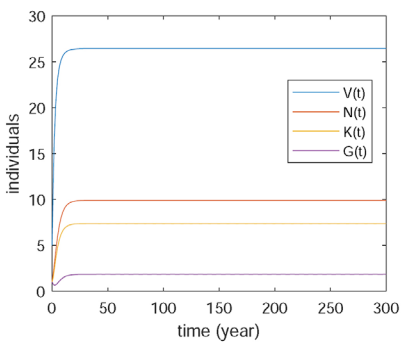

Figure 4

Simulation of model (2.2) with the model inputs in Table 3(ii).

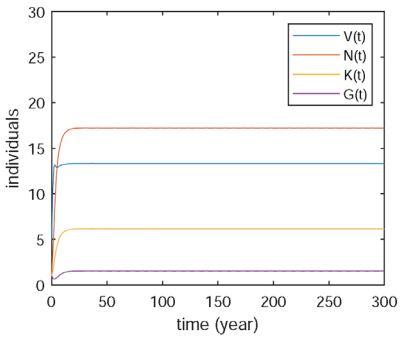

Figure 5

Simulation of model (2.2) with the model inputs in Table 3(iii).

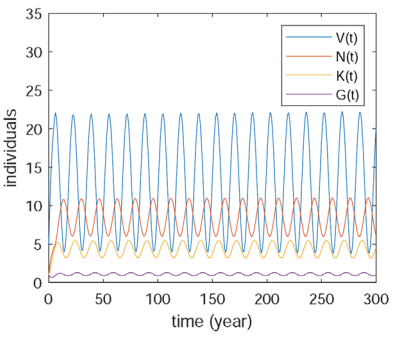

Figure 6

Simulation of model (2.2) with the model inputs in Table 3(iv).

For the model inputs given in Table 3(iv), the corresponding equilibrium point is $P^* = (12.9854,\ 8.4785,\ 4.3387,\ 1.0798)$. Moreover, the corresponding roots of equation (3.7) are $\Phi_1 = 0.1462$, $\Phi_2 = -0.3643$, $\Phi_3 = -0.2794$, and $\Phi_4 = -0.1036$. Conditions (H3) and (H4) are satisfied, where the critical delay $\tau_0 = 5.8379$ and $f_1 f_3 + f_2 f_4 = 0.008 > 0$. According to Theorem 2(ii), a Hopf bifurcation occurs and a limit cycle arises from the equilibrium point P^* (see Figure 6).

4. Sensitivity analysis of the equilibrium point

In this section, the normalized forward sensitivity indices (NFSIs) of the equilibrium point with respect to every model input are calculated. The set of model outputs is given by

$$\mathbf{x} = \{V^*, N^*, K^*, G^*\}.$$

The set of model inputs is given by

$$\mathbf{y} = \{\Psi, \mu, \xi, \sigma, \varepsilon, \kappa, \varpi, \gamma, \beta, \theta, \omega, \chi, \Omega, \nu, \delta, \alpha, \eta, \rho, \phi, N_0, K_0, G_0, \tau\}.$$

Mathematically, the NFSI of an arbitrary model output x_m with respect to an arbitrary model input y_n is given by

$$\Upsilon_{y_n}^{x_m} = \frac{y_n}{x_m}\frac{\partial x_m}{\partial y_n}, \tag{4.1}$$

where $m = 1, 2, 3, 4,$ and $n = 1, \ldots, 23$. Equation (4.1) is one at a time method because the other model inputs remain unchanged. It is explained as the approximate percentage change in the model output x_m when the model

input y_n increases by 1%. We approximate the partial derivative in equation (4.1) using the centered difference approximation as follows:

$$\frac{\partial x_m}{\partial y_n} \approx \frac{x_m(y_n+\Delta y_n)-x_m(y_n-\Delta y_n)}{2\Delta y_n},$$

where $x_m(y_n+\Delta y_n)$ is the figure of the model output x_m when the model input y_n increases by Δy_n and $x_m(y_n-\Delta y_n)$ is the figure of the model output x_m when the model input y_n decreases by Δy_n. By default, $\Delta y_n = 0.001\times y_n$ [22].

5. Discussion

Here, we consider model (2.2) with the model inputs from Table 4. For the model inputs given in Table 4, the corresponding equilibrium point is $P^* = (1.0906\times10^7,\ 9.1242\times10^5,\ 1.1362\times10^4,\ 651.0135)$. Moreover, the corresponding coefficients of equation (3.7) are $\varphi_1 = 2.004$, $\varphi_2 = 1.0052$, $\varphi_3 = 9.28\times10^{-4}$, and $\varphi_4 = 2.126\times10^{-7}$. Then, condition (H2) is satisfied. According to Theorem 2(i), the equilibrium point P^* is locally asymptotically stable (see Figure 7). As shown in Figure 7, the number of all subpopulations reaches their equilibrium solutions at a long-term prediction.

By performing the sensitivity analysis, we will determine which model inputs are the important and sensitive model inputs to change the equilibrium point P^*. Following equation (4.1) and using the model inputs in Table 4, we present in Table 5 the NFSIs of the equilibrium point P^* with respect to every model input.

Based on the definition of every model input, we exclude the effect of the following model inputs. We exclude the removal- or death-related parameters $(\mu,\xi,\varepsilon,\kappa,\beta,\theta,\nu,\delta)$ because it is unrealistic to alter them. We also exclude the changes in the initial conditions (ϕ,N_0,K_0,G_0) because they do not affect the equilibrium point P^*. We exclude the model inputs Ψ, Ω, and α because it is unrealistic to restrict the demographic expansion in order to control diabetes or diabetes-related complications. Without the birth of new individuals, we would face extinction. For the other model inputs, we sort them based on their magnitude of sensitiveness and their sign in Table 6. The magnitudes and signs of NFSIs for $\Upsilon_{y_n}^{V^*}$ were not given since V^* represents the equilibrium point of women who are non-diabetic.

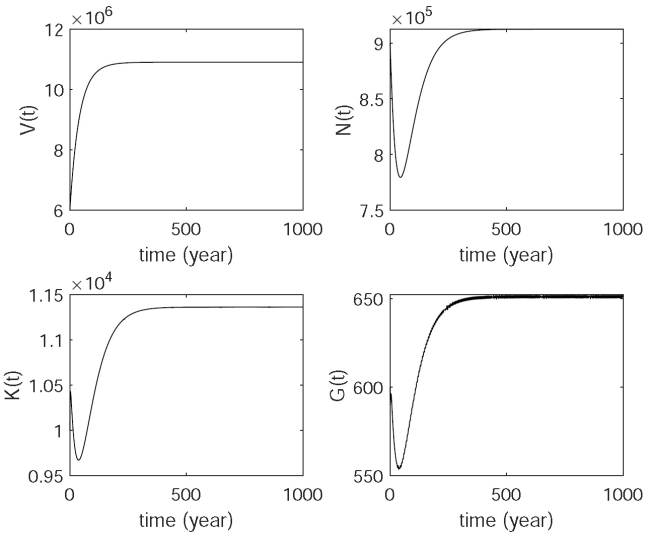

Figure 7

Simulation of model (2.2) with the model inputs in Table 4.

Table 4

Estimated values for the model inputs.

Model input	Value	Source
Ψ	255281	[7]
μ	7.752×10^{-4}	[7]
ξ	0.0218	[7]
σ	1.5831×10^{-3}	[7]
ε	9.9175×10^{-3}	[7]
κ	2.7484×10^{-4}	[7]
ϖ	4679	[7]
γ	0.1228	[7]
β	7.485×10^{-3}	[7]
θ	0.0195	[7]
ω	0.0573	[7]
χ	0.1167	[7]
Ω	0.0108	[7]
ν	0.0202	[7]
δ	1.0292×10^{-3}	[7]

Contd...

α	1.3833×10^{-4}	[7]
η	0.8048	[7]
ρ	0.8503	[7]
ϕ	6000000	Assumed
N_0	900000	[7]
K_0	10000	[7]
G_0	600	[7]
τ	10	[16]

Table 5

The NFSIs of the equilibrium point P^* with respect to every model input using the model inputs in Table .

Model input (y_n)	$\Upsilon_{y_n}^{V^*}$	$\Upsilon_{y_n}^{N^*}$	$\Upsilon_{y_n}^{K^*}$	$\Upsilon_{y_n}^{G^*}$
Ψ	0.9918	0.7428	0.7759	0.7759
μ	–0.0343	–0.0692	–0.0646	–0.0646
ξ	–0.9291	–0.8570	–0.8666	–0.8666
σ	–0.0428	0.7073	0.6074	0.6074
ε	–0.0159	–0.4959	–0.4320	–0.4320
κ	-4.4017×10^{-4}	–0.0137	–0.0120	–0.0120
ϖ	0.0082	0.2572	0.2241	0.2241
γ	-1.341×10^{-4}	0.0035	0.0030	–0.1198
β	-1.6358×10^{-5}	-4.2877×10^{-5}	-3.9346×10^{-5}	–0.0075
θ	-4.2617×10^{-5}	-1.117×10^{-4}	-1.025×10^{-4}	–0.0196
ω	-1.8404×10^{-5}	1.3425×10^{-4}	–0.0547	0.9453
χ	–0.0023	0.0581	–0.0615	–0.0615
Ω	0.0176	–0.4516	0.4777	0.4777
ν	-7.7701×10^{-4}	–0.0020	–0.0211	–0.0211
δ	-3.9589×10^{-5}	-1.0049×10^{-4}	–0.0011	–0.0011
α	-5.0701×10^{-4}	0.0092	0.1411	0.1411
η	0.0031	–0.0562	–0.8616	–0.8616
ρ	1.9308×10^{-4}	–0.0033	–0.0029	–0.8531
ϕ	0	0	0	0
N_0	0	0	0	0
K_0	0	0	0	0
G_0	0	0	0	0
τ	–0.0055	–0.1710	–0.1490	–0.1490

Table 6

Magnitude and sign of the NFSIs of N^*, K^*, and G^* using the model inputs in Table 4.

(A) NFSIs of N^*				(B) NFSIs of K^*				(C) NFSIs of G^*		
y_n	$\lvert \Upsilon_{y_n}^{N^*} \rvert$	sign		y_n	$\lvert \Upsilon_{y_n}^{N^*} \rvert$	sign		y_n	$\lvert \Upsilon_{y_n}^{N^*} \rvert$	sign
σ	0.7073	+		η	0.8616	–		ω	0.9453	+
ϖ	0.2572	+		σ	0.6074	+		η	0.8616	–
τ	0.1710	–		ϖ	0.2241	+		ρ	0.8531	–
χ	0.0581	+		τ	0.1490	–		σ	0.6074	+
η	0.0562	–		χ	0.0615	–		ϖ	0.2241	+
γ	0.0035	+		ω	0.0547	–		τ	0.1490	–
ρ	0.0033	–		γ	0.003	+		γ	0.1198	–
ω	0.0001	+		ρ	0.0029	–		χ	0.0615	–

From Table 6(A), the most sensitive model input that increases the equilibrium solution of women who are diabetics (N^*) is the rate of developing diabetes (σ). From Table 6(B), the most sensitive model input that decreases the equilibrium solution of women with gestational diabetes (K^*) is the rate of women with gestational diabetes becoming non-diabetic after puerperium (η). From Table 6(C), the most sensitive model input that increases the equilibrium solution of women with gestational diabetes and complications (G^*) is the rate of women with gestational diabetes developing diabetes-related complications (ω).

One of the ways to simultaneously decrease σ and increase η is through prevention and education. Primary intervention should be targeted at women early in their childbearing age to ward off diabetes during pregnancy. Before making any arrangements to conceive, women at risk of gestational diabetes should receive information about the management plans and risks of pregnancy. To avoid the complications associated with diabetes during pregnancy, screening of women with gestational diabetes should continue. Controlling the model input ω requires treatment of the diabetes-related complications during pregnancy to avoid mortality and ensure their glycemic levels return to normal after the pregnancy. Considering the sensitive model inputs and other essential elements like money spent, logistics, labor force, time, accessibility, and other factors, the rankings of model inputs may help policymakers decide on the best intervention measures.

6. Conclusion

In this work, we considered a delay differential equation (DDE) system for the population dynamics of gestational diabetes. We have investigated the condition that should be satisfied for the non-negativity of the solution for all time. Regarding the parameter τ being considered as the bifurcation parameter, we studied the occurrence of periodic orbits. We proved that when certain conditions are satisfied, the equilibrium point P^* may be locally asymptotically stable for $\tau \geq 0$, a Hopf bifurcation occurs at a critical delay $\tau = \tau_0$ (a family of periodic orbits bifurcates from P^*), or becomes unstable for $\tau > \tau_0$. The theoretical findings are confirmed through numerical simulations. It is noticeable that for the same model without time delay, Mat Daud et al. [7] showed that an oscillatory solution does not occur. The sensitivity analysis results also showed that the gestational diabetes results might depend on multiple crucial aspects represented by the sensitive model inputs. Simplifying the visualization of the relationship between disease outcomes and various factors could aid policymakers in making informed decisions. This model will offer a useful tool for community welfare management and surveillance, such as estimating the efficacy of intervention programs and anticipating future incidence and burden of gestational diabetes.

Acknowledgment

Thanks to Associate Professor Dr. Auni Aslah bin Mat Daud from Universiti Malaysia Terengganu for the financial support provided during the second author's doctoral studies, which was funded by the Ministry of Higher Education, Malaysia and the Fundamental Research Grant Scheme (grant number 59523, FRGS/1/2018/STG06/UMT/02/2).

References

[1] Rajab, K. E., Issa, A. A., Hasan, Z. A., Rajab, E. and Jaradat, A. A. Incidence of gestational diabetes mellitus in Bahrain from 2002 to 2010. *International Journal of Gynecology & Obstetrics,* 117(1): 74-77 (2012).

[2] Buckley, B. S., Harreiter, J., Damm, P., Corcoy, R., Chico, A., Simmons, D., Vellinga, A., Dunne, F. and DALI Core Investigator Group. Gestational diabetes mellitus in Europe: prevalence, current screening practice and barriers to screening. A review. *Diabetic medicine,* 29(7): 844-854 (2012).

[3] Fraser, A. and Lawlor, D. A. Long-term health outcomes in offspring born to women with diabetes in pregnancy. *Current Diabetes Reports*, 14: 459 (2014).

[4] Mackin, S. T., Nelson, S. M., Kerssens, J. J., Wood, R., Wild, S., Colhoun, H. M., Leese, G. P., Philip, S. and Lindsay, R. S. Diabetes and pregnancy: national trends over a 15 year period. *Diabetologia*, 61(5): 1081-1088 (2018).

[5] Plows, J. F., Stanley, J. L., Baker, P. N., Reynolds, C. M. and Vickers, M. H. The pathophysiology of gestational diabetes mellitus. *International Journal of Molecular Sciences*, 19(11): 3342 (2018).

[6] Lohse, N., Marseille, E. and Kahn, J. G. Development of a model to assess the cost-effectiveness of gestational diabetes mellitus screening and lifestyle change for the prevention of type 2 diabetes mellitus. *International Journal of Gynecology & Obstetrics*, 115(S1): S20-S25 (2011).

[7] Mat Daud, A. A., Toh, C. Q., and Saidun, S. Development and analysis of a mathematical model for the population dynamics of diabetes mellitus during pregnancy. *Mathematical Models and Computer Simulations*, 12(4): 620-630 (2020).

[8] Sun, G. Q. Mathematical modeling of population dynamics with Allee effect. *Nonlinear Dynamics*, 85: 1-12 (2016).

[9] Levy, J., Gavin III, J. R., Scott, M.J. and Avioli, L. V. Mineral homeostasis in neonates of streptozotocin-induced noninsulin-dependent diabetic rats and in their mothers during pregnancy and lactation. *Bone*, 8(1): 1-6 (1987).

[10] Nasir, H. and Mat Daud, A. A. Population models of diabetes mellitus by ordinary differential equations: a review. *Mathematical Population Studies*, 29(3): 95-127 (2022).

[11] Nasir, H. Stability analysis and optimal control of a five-state diabetic population model. *Journal of Statistics and Management Systems*, 25(1): 245-267 (2022).

[12] MacDonald, N. *Time lags in biological models (Vol. 27)*. Springer Science & Business Media (2013).

[13] Hutchesson, M. J., De Jonge Mulock Houwer, M., Brown, H. M., Lim, S., Moran, L. J., Vincze, L., Rollo, M. E., and Hollis, J. L. Supporting women of childbearing age in the prevention and treatment of overweight and obesity: a scoping review of randomized control trials of behavioral interventions. *BMC Women's Health*, 20: 14 (2020).

[14] Smith, K. and Lipari, R. Women of childbearing age and opioids. *The CBHSQ report* (2017).

[15] Khetan, A. K. and Rajagopalan, S. Prediabetes. *Canadian Journal of Cardiology*, 34(5): 615-623 (2018).

[16] Nasir, H. On the dynamics of a diabetic population model with two delays and a general recovery rate of complications. *Mathematics and Computers in Simulation*, 200: 571-602 (2022).

[17] Driver, R. D. *Ordinary and Delay Differential Equations (Vol. 20)*. Springer Science & Business Media (2012).

[18] Allen, L. J. S. *Introduction to Mathematical Biology*. Pearson/Prentice Hall (2007).

[19] Rocha, D., Silva, C. J. and Torres, D. F. Stability and optimal control of a delayed HIV model. *Mathematical Methods in the Applied Sciences*, 41(6): 2251-2260 (2018).

[20] Mohabati, F. and Molaei, M. Bifurcation analysis in a delay model of IVGTT glucose-insulin interaction. *Theory in Biosciences*, 139(1): 9-20 (2020).

[21] Smith, H. L. *An Introduction to Delay Differential Equations with Applications to the Life Sciences*. Volume 57 (Springer, 2011) (2011).

[22] Zi, Z., Zheng, Y., Rundell, A.E. and Klipp, E. SBML-SAT: a systems biology markup language (SBML) based sensitivity analysis tool. *BMC Bioinformatics*, 9(1): 342 (2008).

Received October, 2022